

Optical microsystem design and fabrication for medical image magnification

C. G. Costa¹ · J. M. Gomes¹ · R. F. Wolffenbuttel² · J. H. Correia¹

Received: 3 August 2015 / Accepted: 8 January 2016
© Springer-Verlag Berlin Heidelberg 2016

Abstract Medical imaging is an important part of diagnosis. The procedure should provide valuable information for diagnosis and, at the same time, should be minimally invasive for the patient. Therefore, when performing endoscopic imaging, a system with reduced dimensions is crucial. The performance of imaging systems, used in several diagnosis endoscopic procedures, would highly benefit from the integration of an imaging magnification optical microsystem (IMOM) able to perform *in vivo* and real-time tissue microscopy. This paper proposes a miniaturized IMOM: its total length is 12.164 mm and has a lateral lens assembly of 3.894 mm. A microfabricated PDMS lens was included in the system, obtained by a hanging droplet approach, a very low-cost and effective method. A paraxial magnification of 4–14 times was achieved with a good performance in every optical analysis evaluated. A modulation transfer function around 38 % at 50 lp/mm was obtained and maximum distortion about 1.8 %.

1 Introduction

The need to inspect the human body's cavities goes back to the Greek civilization, where the earliest references to endoscopy were made by Hippocrates, describing a rectal speculum. Throughout the centuries, the scientific evolution

made possible to go from the first speculums to high resolution video-endoscopes, used today. Endoscopic imaging enables a real-time image from the inside of the human body, bringing crucial information to accurate diagnosis.

The procedure is minimally invasive by using the body cavities, or small incisions, to access the organ of interest and obtain images of its condition. It can be used in different medical fields: cystoscopy, has been used to inspect the bladder, gastroscopy names the procedure applied in the stomach and duodenum, bronchoscopy is performed to image the lungs and even in ophthalmology this procedure is useful.

For confirming a suspicious image diagnosis, a histopathological examination is necessary. This requires obtaining a tissue sample for an *ex vivo* analysis. Despite being the standard procedure, biopsy histopathological diagnosis has some limitations: it is an invasive procedure that needs the resection of the tissue to be analyzed. The sampling of the tissue is also a concern since it is necessary to remove the appropriate tissue from the patient (Liu et al. 2011).

Recent developments in optical imaging technologies have established new diagnosis features, enabling high-resolution, minimally invasive and real-time imaging. This can lead to new “optical biopsy”, performed *in situ* and in real-time (Li and Grundfest 2012). High magnification endoscopy is among the most relevant advancements in endoscopic imaging in the recent time. In the examination of doubtful tissue alterations, magnification endoscopy allows the study of the tissue architecture and recognition of the affected mucosa with great precision. This information can be used to differentiate affected tissue from healthy neighboring tissues and to judge the severity of the infection. Moreover, magnification endoscopy can be a tool to assist histopathology, since it can be used to perform image-guided biopsies identifying tissue sites of greatest concern.

✉ C. G. Costa
cgcosta@dei.uminho.pt

¹ CMEMS-UMinho, Department of Industrial Electronics, University of Minho, Campus Azurem, 4800-058 Guimarães, Portugal

² Faculty of EEMCS, TUDelft, Mekelweg 4, 2628 CD Delft, The Netherlands

This can reduce the number of samples and increase the accuracy of the procedure (Liu et al. 2011).

In this paper it is proposed an imaging magnification optical microsystem (IMOM) of reduced dimensions that can be integrated in several medical devices, even wireless ones, since it was designed to create the magnified image in the sensor included in the device. The proposed system can be considered a highly miniaturized digital microscope, with which in vivo tissue microscopy can be performed in real-time.

2 Specifications and optical design

Optical design of a miniaturized IMOM is a real challenge. The extent to which the dimensions of this module can be reduced is a tradeoff between the overall device length, transverse magnification and image quality of the optical system. The small structures in the biological tissue aimed to be visualized in endomicroscopy images define the object's height, which in this case was defined as 200 μm . CMOS image sensors can be considered for the IMOM and its diagonal defines the image height. Considering these restrictions, an optimized solution for the optical design was obtained.

The proposed design was optimized and evaluated using ZEMAX[®] optical software. A side-view arrangement, perpendicular to the tissue was chosen, allowing a close contact with the in vivo samples. The primary wavelength selected in the simulation was 550 nm, which is the central wavelength of the LED white light considered as illumination.

Table 1 presents the lens data that defines the system: radii, thicknesses, glasses, semi-diameters and conic constant of each surface.

In surface 10 is inserted a non-sequential component (NSC) to simulate the prism used to reflect the light rays into the imaging sensor. This surface acts as an entry port to the non-sequential ambient. The parameters that define the NSC are described in the non-sequential component editor, shown in Table 2.

Figure 1 shows the 2D schematic of the lens system and the 3D model of the IMOM. The first surface is the optical dome. It is a plane surface of poly(methyl methacrylate) (PMMA), $n_d = 1.49$, that will be in direct contact with the object, which is the tissue under examination. The first lens in the system is a commercial lens of dense lanthanum flint glass (LaSFN₉), (Opstosigma[®], 011-0020, $f_1 = 1$ mm), with high refractive index ($n_d = 1.85$), leaning against the dome. The next surface is a similar lens, but with different radius (Opstosigma[®], 011-0070, $f_2 = 3$ mm). After that, an aperture stop with a diameter of 0.6 mm was included. For focusing purposes a converging meniscus is a good solution for the following lens in the system. To produce this effect, a plano-concave configuration was selected (Opstosigma[®], 015-0020, $f_3 = -4$ mm). Next, a fourth lens was included, directly on third lens' flat surface, with a plano-convex configuration, and it was designed to be manufactured with polydimethylsiloxane (PDMS). This was the chosen material due to its optical properties, such as optical transparency in visible region and a well-documented fabrication process (Miao and Wang 2014).

PMDS was included in the ZEMAX[®] Glass Catalog based in the Sellmeier formula established by (Cai 2008) and presented in Eq. (1), where n represents the refractive

Table 1 Lens data of the IMOM optical system

Surface	Type	Comment	Radius (mm)	Thickness (mm)	Glass	Semidiameter (mm)	Conic
OBJ	Standard	Optical dome	Infinity	0.530	PMMA	0.100	0.000
1	Standard	1st lens	Infinity	0.800	LaSFN ₉	0.750	0.000
2	Standard		-0.850	0.000		0.750	0.000
3	Standard	2nd lens	2.570	1.300	LaSFN ₉	1.000	0.000
4	Standard		Infinity	0.100		1.000	0.000
STO	Standard	Aperture stop	Infinity	0.100		0.300	0.000
6	Standard	3rd lens	-3.400	0.800	LaSFN ₉	1.000	0.000
7	Standard		Infinity	0.000		1.000	0.000
8	Standard	4th lens	Infinity	0.264	PDMS	1.000	0.000
9	Even asphere		-1.500	0.300		1.000	-4.000
10	Non-sequential component	Prism	Infinity	-	-	0.443	0.000
11	Standard		Infinity	8.664		1.000	0.000
IMA	Standard	Image sensor	Infinity	-		1.557	0.000

Table 2 Non-sequential component editor for defining the prism

Object type	Comment	X position	Y position	Z position	Tilt X	Tilt Y	Tilt Z	Material	X1 Half with	Y1 half with	Z length	X2 half with	Y2 half with	Rear Y angle
Rectangular volume	Prism	0	-1.5	1.5	-90	0	0	N-BK7	1.5	1.5	1.5	1.5	1.5	45

index and λ is the wavelength. According to this dispersion formula the refractive index of the PDMS is $n_d = 1.38$.

$$n^2 = 1 + \frac{-2.30744 \times \lambda^2}{\lambda^2 + 0.02605} + \frac{1.85952 \times \lambda^2}{\lambda^2 + 0.01362} + \frac{1.39944 \times \lambda^2}{\lambda^2 + 0.01349} \tag{1}$$

An optical system structure can be greatly simplified and the image quality significantly improved with aspheric technology. To improve the system performance a plano-convex configuration with an aspheric surface was idealized to the fourth lens. The main reason for using aspheric components is for reducing spherical aberration, particularly because in this design there is a constraint on the number of optical surfaces.

A spherical surface is defined only by one parameter, the radius of curvature of the surface. On the other hand, in aspheric surfaces its localized curvature changes across the surface and therefore it cannot be defined with only one curvature over the entire surface (Fischer et al. 2000). An aspheric surface is defined by the sag or z-coordinate, z , which is given by Eq. (2).

$$z = \frac{cr^2}{1 + \sqrt{1 - (1 + k)c^2r^2}} + \sum a_i r^{2i} \tag{2}$$

where c is the base curvature at the vertex, k is a conic constant, r is the radial coordinate measured perpendicularly from the optical axis, and $a_i r^{2i}$ are the higher-order aspheric terms. Therefore, the sag is the z-component of the displacement of the surface from the vertex, at distance r . When the higher-order aspheric terms are zero, the aspheric surface takes the form of a rotationally symmetric conic cross section with the sag defined as the first term of Eq. (2) (Fischer et al. 2000). In this design the aspheric surface has a conic constant $k = -4$, which means it is a hyperboloid surface. A hyperboloid forms an aberration-free image for conjugates on two different sides of the surface (Fischer et al. 2000). The surface radius is 1.5 and is 0.264 mm thick.

An N-BK7 ($n_d = 1.52$) right-angle prism with a reflective surface at 45° was included in the optical system (Thorlabs®, PS905), so that the image would be formed on the image sensor. The prism’s material provides an excellent transmittance in the visible spectrum, around 92 %.

3 System design analysis

The system’s effective focal length (EFL) and the working f -number are -0.889 mm and 18.216, respectively. The paraxial magnification is 13.929. Total track (TOTR), length of the optical system measured by the vertex separations between the left and right limits, is 12.164 mm, and

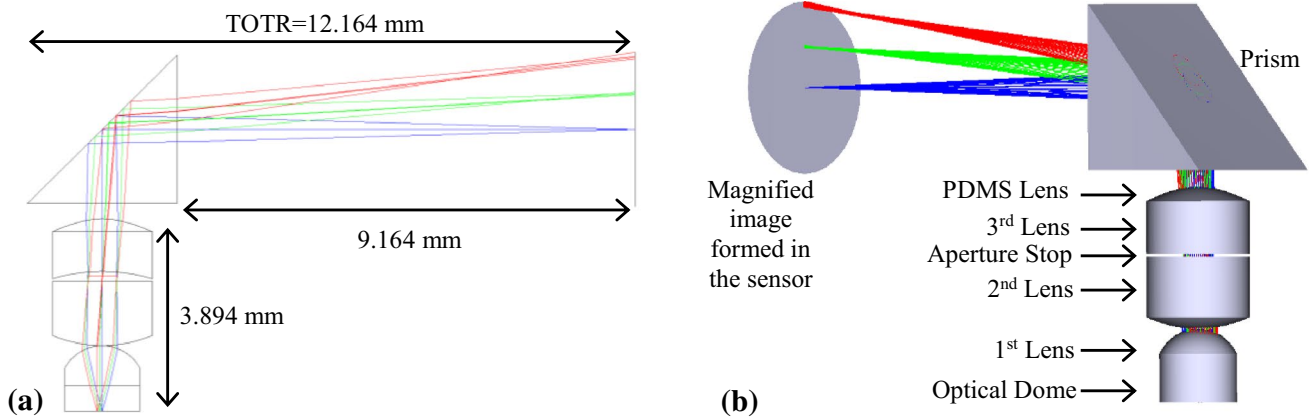
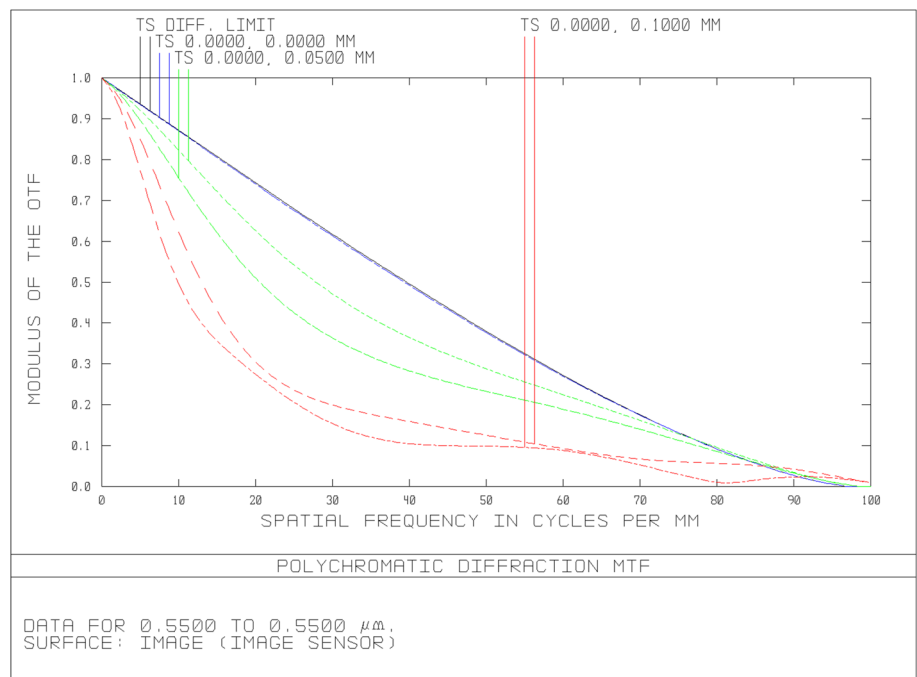


Fig. 1 **a** IMOM optical system layout and dimensions, *TOTR* total track of the system. **b** 3D model of the proposed IMOM

Fig. 2 Modulation transfer function of the IMOM optical system



the lateral lens assembly is 3.894 mm in length. The distance between the prism and the image sensor is 9.164 mm. In order to evaluate the image quality several analysis were performed.

Figure 2 shows the modulation transfer function (MTF) of the system. MTF is a measure of how well the original contrast of the object is transferred to the image and is expressed in percentage as a function of the spatial frequency. The modulation transfer decreases with increasing spatial frequency (Fischer et al. 2000). The MTF produced by the larger field of view (FOV) at 50 lp/mm is about 9.88 % for the tangential rays and 12.5 % for sagittal ones. For the central FOV the MTF is nearly 37.6 % at 50 lp/mm, for both the tangential and sagittal rays.

In Fig. 3 is shown the spot diagram for this optical system. It is the geometrical image blur formed by the lens system when imaging a point object. The diameter of the Airy disk is 12.22 μm. Root-mean-square (rms) spot diameter is the diameter of a circle containing approximately 68 % of the energy. The rms radius of the spot size for the three fields in the simulation are 1.23, 24.52 and 54.03 μm. The geometric radius of the spot size has a maximum of 138.05 μm for the exterior field.

Figure 4 presents the field curvature and distortion. The locations of the tangential *T* and sagittal *S* foci are plotted for a full range of field angles. Figure 5 shows the grid distortion of the proposed optical design. The term distortion refers to a change in the geometric representation of an

Fig. 3 Spot diagram analysis for three field positons

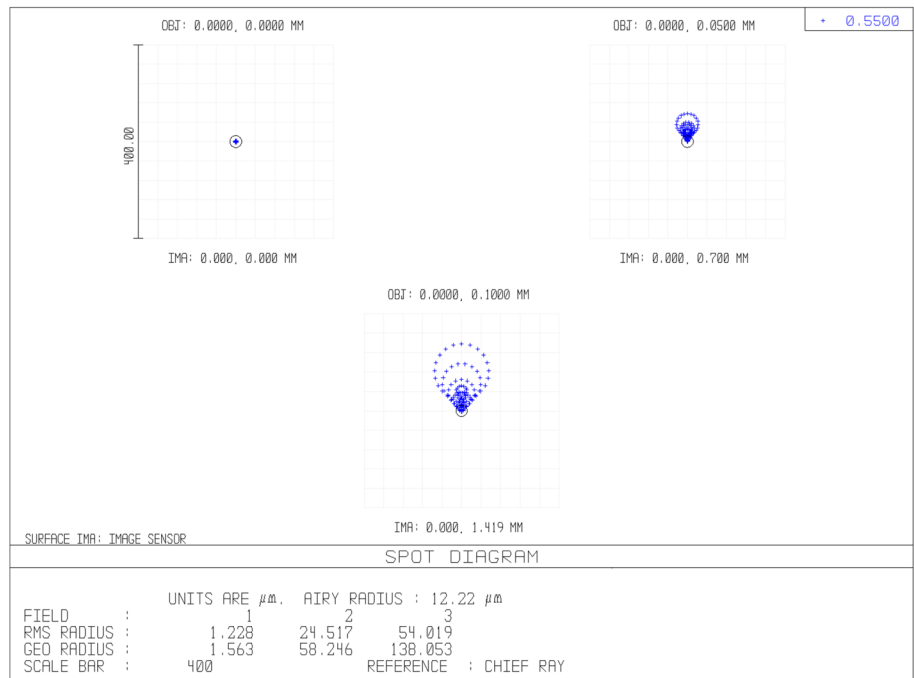
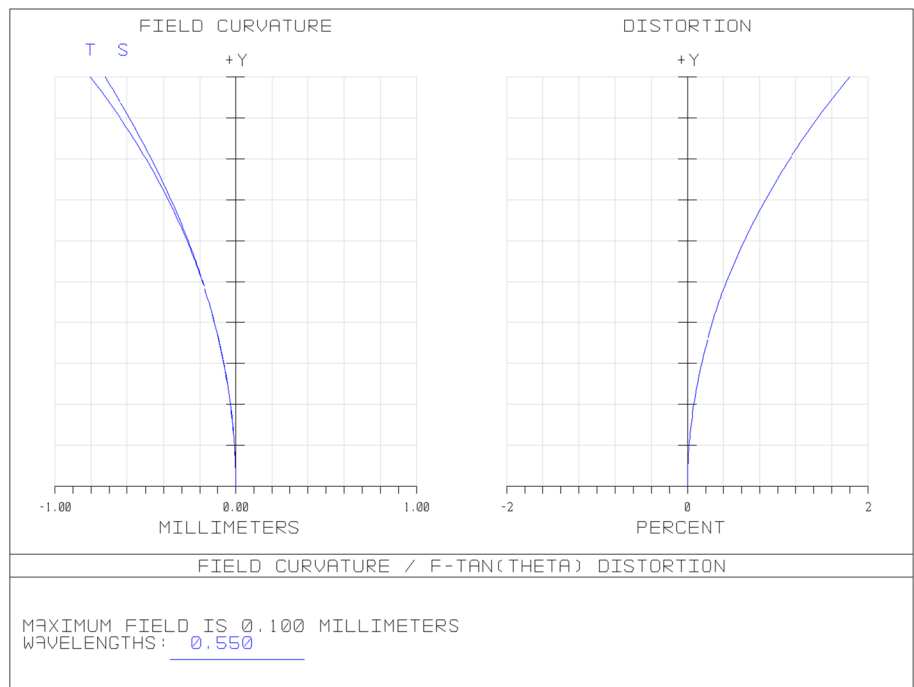


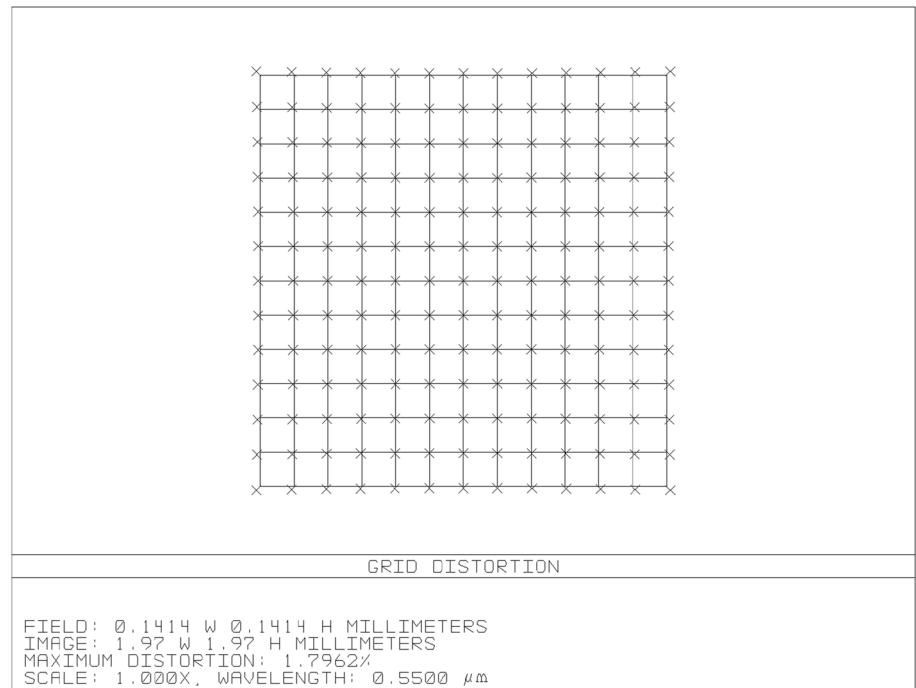
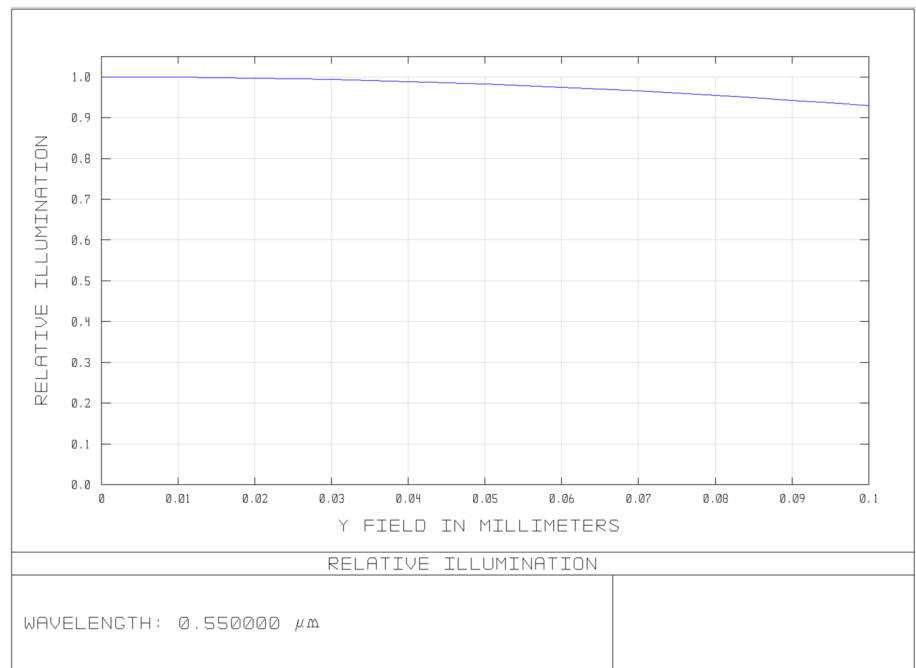
Fig. 4 Field curvature



object in the image plane. The largest distortion is 1.796 %, which reveals a very small pincushion distortion.

The system’s relative illumination (RI) was also evaluated. It defines the intensity of illumination per unit area of image surface. Figure 6 shows the relative illumination plot from the optical axis to the largest field defined. This reveals a RI of 93 % for the largest field.

Figure 7 presents the OPD (Optical Path Difference) fan, which displays the difference between the optical path length of the ray and the optical path length of the chief ray, for each evaluated field. A system without aberration would show a straight line coinciding with the x-axis. For this optical system the wave aberration is about five times the wavelength, at the most exterior field, but can be neglected for the central FOV.

Fig. 5 Grid distortion**Fig. 6** Relative illumination

4 PDMS lens fabrication and characterization

An optical lens contributes to the efficiency of an optical system by enabling the convergence and focusing of the light onto the sensor active area. By using simple and low-cost lens fabrication techniques it is possible to assemble an optical system compatible with a multitude of applications.

The presented IMOM integrates a custom-made lens with theoretical values of 1 mm, 264 μm and 4.0138 mm for the semi-diameter, thickness and EFL, respectively, and conic constant $k = -4$. However, because of fabrication constraints some adaptations to the design were considered.

For testing the fabrication method, a spherical lens was produced. This lens has the same radius, focal length and

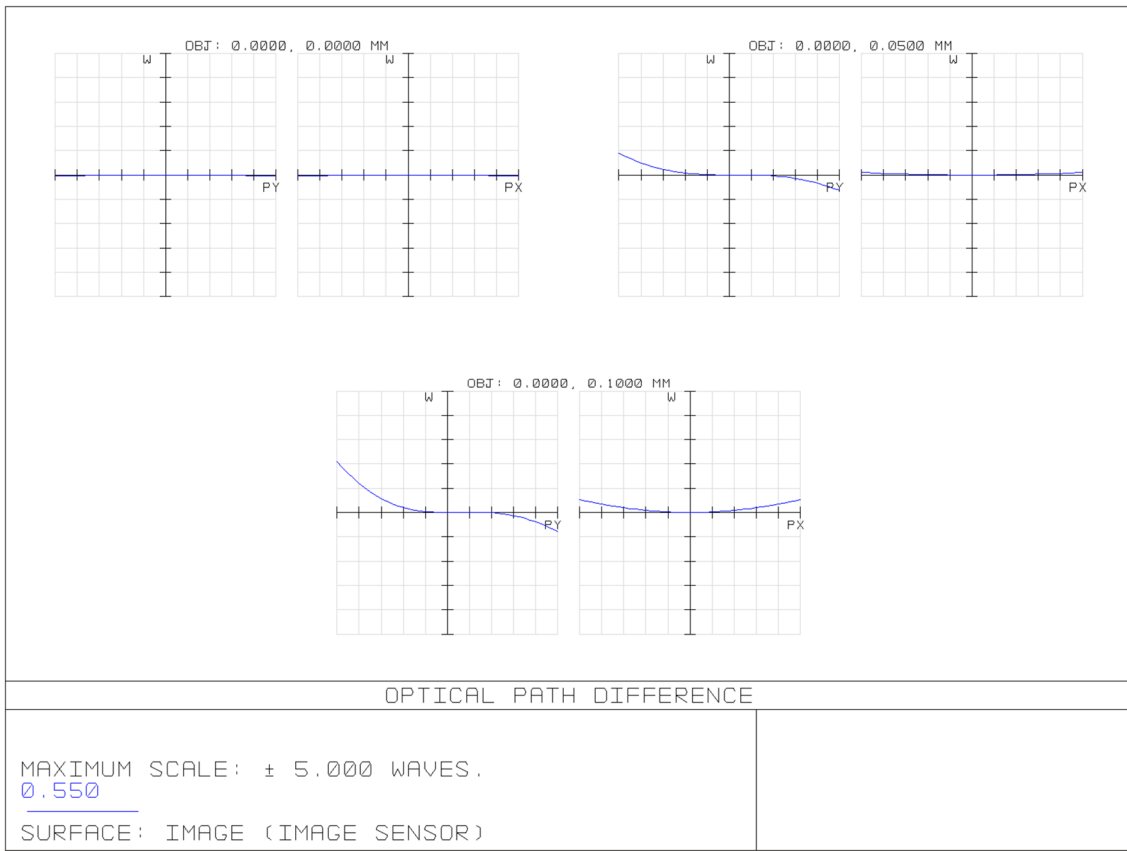
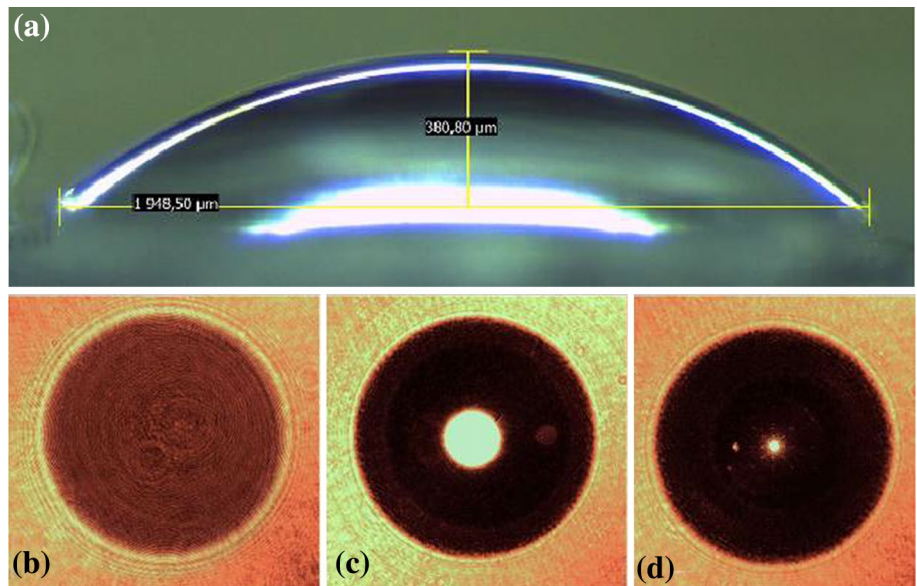


Fig. 7 OPD fan

Fig. 8 **a** PDMS fabricated lens. **b–d** Light beam focusing procedure from unfocused to focused, for determining the lens focal length



semi-diameter as initially designed, but its thickness was recalculated to respond to a spherical design. The new thickness is 382 μm, with $k = 0$.

The lens in Fig. 8a was fabricated in PDMS using a hanging droplet method approach, where a controlled droplet volume of PDMS is placed on a substrate and cured

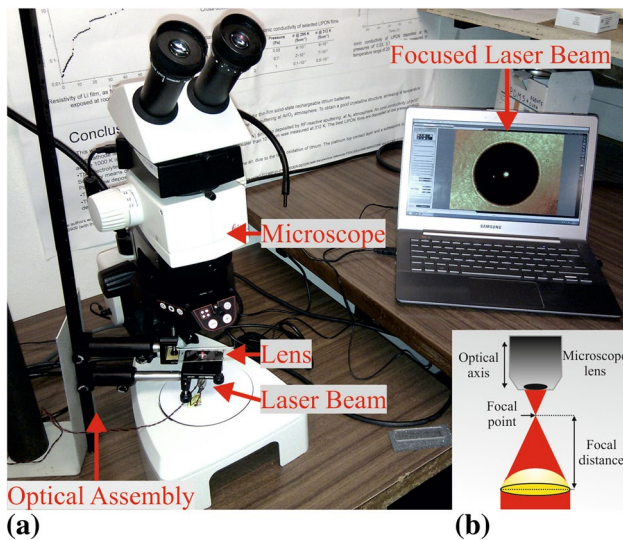


Fig. 9 a Setup for determining the lens' focal length. b Schematic

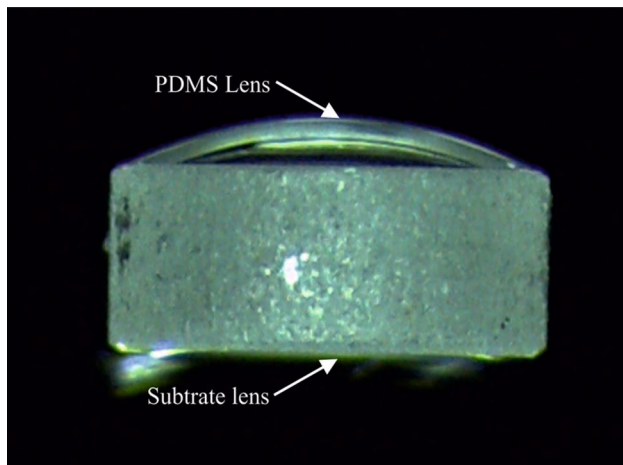


Fig. 10 PDMS lens profile, fabricated on top of the plano-concave glass lens

inverted, resulting in a lens with final dimensions very close to the calculated values. Therefore, it was proved that the fabrication method was significantly accurate. Figure 8b–d show the successive lens focusing procedure for determining the actual focal length.

The focal length measurements were performed with the setup presented in Fig. 9. A constricted light spot is created by a 635 nm collimated round laser light beam passing through the lens. The measurement starts by focusing

the microscope image on the lens plane for establishing the distance reference and then shifted on the optical axis, until the most constricted beam spot is observed. The distance between the two points equals the lens focal length. The measured focal length confirmed the calculated values, proving the feasibility of this method.

Due to the PDMS adhesion and internal cohesion it is possible to fixate the lens radius at 1 mm by fabricating directly on the planar side of the rigid lens, with the same radius. This approach ensures that the droplet volume only physically affects the lens height, thus its curvature. Moreover, the rigid lens serves also as substrate making unnecessary further fixating mechanisms.

Figure 10 shows the adhesion of the PDMS lens to the plano-concave glass lens.

5 IMOM integration and testing

After fabrication, validation of the technique and focal length measurements of the PDMS lens, it was necessary to study a solution to integrate the complete lens system and the image sensor, in order to obtain the desired IMOM.

A computer-aided design (CAD) model was designed taking into account the system's dimensions, spacing and alignment. The project is shown in Fig. 11a. The lenses are presented in their correct position and configuration, followed by the prism. The spacing between the lenses and between the prism and the image sensor was projected to respond to the simulation's data, presented in Sect. 2. A solution to include the illumination source into the IMOM was also considered. The white LEDs were integrated into a PCB (printed circuit board) next to the image sensor and the light path were included in the lens holder model, so that the illumination could be applied onto to the tissue without causing saturation on the sensor.

Based on the CAD design the lens holder was obtained by 3D printing of modular pieces. In Fig. 11b is presented the final lens holder assembly.

After the fabrication of the lens holder and integration of all optical system's components, experimental imaging tests were performed. Figure 12 shows the magnified images acquired with a 2.56×2.56 mm CMOS imager and obtained with the proposed IMOM. The images reveal good magnification ability, around $4\times$, and satisfying objects distinction.

Further improvements can be made to this system, such as an auto-focusing actuator to perform adaptive magnification, as proposed by (Song et al. 2010).

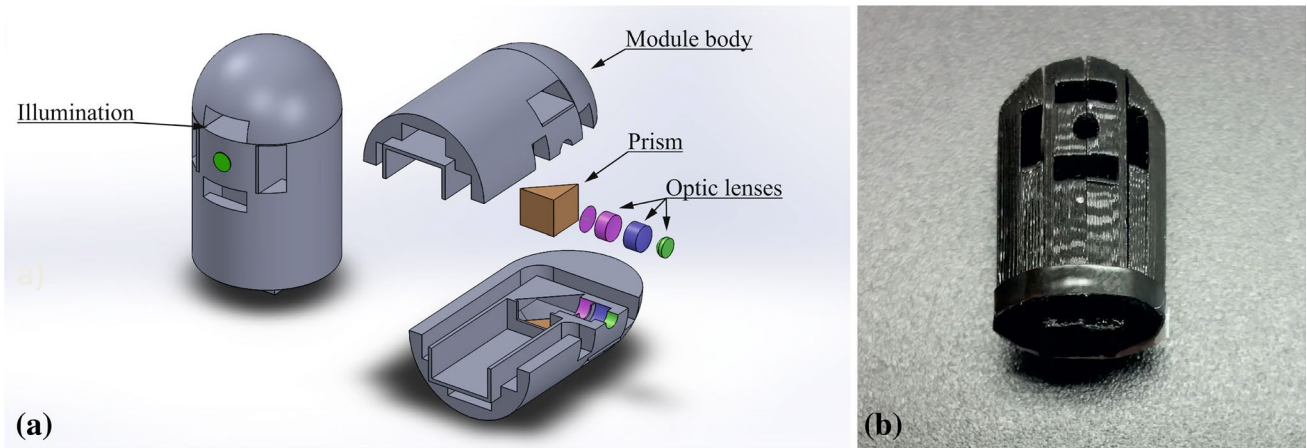


Fig. 11 **a** CAD design of the lenses holder. **b** Lens holder prototype obtained by 3D printing



Fig. 12 Magnified images obtained with the IMOM proposed (4× magnification)

6 Conclusion

The IMOM optical system presented has a simple structure, low-cost integration and a satisfactory image quality. Its reduced dimensions made it suitable to be included in several medical devices, improving the patient comfort and allowing high magnification (4–14×) of suspicious tissues. The side-view configuration provides great advantages to obtain images in direct contact with the sample and thus offer small object distance. This improves the image quality and allows higher magnification values. The integration of a custom made PDMS lens improved the systems performance. Its fabrication was demonstrated with positive results for lens dimensions and focal length.

Acknowledgments This research was supported by Marie Curie Intra European Fellowship within the 7th European Community Framework Programme.

References

- Cai DK (2008) Optical and mechanical aspects on polysiloxane based electrical-optical-circuits-board. Ph. D thesis, Dortmund University of Technology
- Fischer R, Tadic-Galeb B, Yoder P, Galeb R (2000) Optical system design, 2nd edn. McGraw-Hill, New York
- Li X, Grundfest WS (2012) Endomicroscopy technologies and biomedical applications. *J Biomed Opt* 17(2):021101
- Liu JTC, Loewke NO, Mandella MJ, Levenson RM, Group C (2011) Point-of-care pathology with miniature microscopes. *Anal Cell Pathol* 34:81–98
- Miao Z, Wang W (2014) Design and fabrication of microlens arrays as beam relay for free-space optical interconnection. *Microsyst Technol* 20(10–11):1843–1847
- Song BY, Nam DS, Kim JG, Park JS, Lee JY, Shin KS, Lee J (2010) Auto-focusing actuator and camera module including flexible diaphragm for mobile phone camera and wireless capsule endoscope. *Microsyst Technol* 16(1–2):149–159